

University of Alabama in Huntsville

**LOUIS**

---

Theses

UAH Electronic Theses and Dissertations

---

2021

## Experimental measurements of the wing deformation and force production of real monarch butterfly wings

Timothy Daniel Robert Morris

Follow this and additional works at: <https://louis.uah.edu/uah-theses>

---

### Recommended Citation

Morris, Timothy Daniel Robert, "Experimental measurements of the wing deformation and force production of real monarch butterfly wings" (2021). *Theses*. 697.  
<https://louis.uah.edu/uah-theses/697>

This Thesis is brought to you for free and open access by the UAH Electronic Theses and Dissertations at LOUIS. It has been accepted for inclusion in Theses by an authorized administrator of LOUIS.

**EXPERIMENTAL MEASUREMENTS OF THE WING  
DEFORMATION AND FORCE PRODUCTION OF REAL  
MONARCH BUTTERFLY WINGS**

**by**

**TIMOTHY DANIEL ROBERT MORRIS**

**A THESIS**

**Submitted in partial fulfillment of the requirements  
for the degree of Master of Science in Engineering  
in  
The Department of Mechanical and Aerospace Engineering  
to  
The School of Graduate Studies  
of  
The University of Alabama in Huntsville**

**HUNTSVILLE, ALABAMA**

**2021**

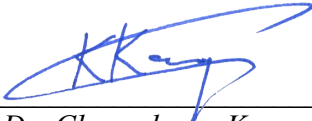
In presenting this thesis in partial fulfillment of the requirements for a master's degree from The University of Alabama in Huntsville, I agree that the Library of this University shall make it freely available for inspection. I further agree that permission for extensive copying for scholarly purposes may be granted by my advisor or, in his/her absence, by the Chair of the Department or the Dean of the School of Graduate Studies. It is also understood that due recognition shall be given to me and to The University of Alabama in Huntsville in any scholarly use which may be made of any material in this thesis.


Timothy Morris      Nov 8, 2021  
(student signature)      (date)

# THESIS APPROVAL FORM

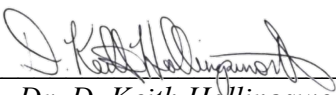
Submitted by Timothy Daniel Robert Morris in partial fulfillment of the requirements for the degree of Masters of Science in Mechanical Engineering and accepted on behalf of the Faculty of the School of Graduate Studies by the thesis committee.

We, the undersigned members of the Graduate Faculty of The University of Alabama in Huntsville, certify that we have advised and/or supervised the candidate on the work described in this thesis. We further certify that we have reviewed the thesis manuscript and approve it in partial fulfillment of the requirements for the degree of Master of Science in Engineering.

  
\_\_\_\_\_  
*Dr. Chang-kwon Kang* 11/7/2021 Committee Chair  
(Date)

  
\_\_\_\_\_  
*Dr. Farbod Fahimi* 11/8/2021  
(Date)

  
\_\_\_\_\_  
*Dr. Kyung-ho Roh* 11/8/2021  
(Date)

  
\_\_\_\_\_  
*Dr. D. Keith Hollingsworth* 12/1/2021 Department Chair  
(Date)

  
Shankar Mahalingam Digitally signed by Shankar Mahalingam  
Date: 2021.12.15 15:43:05 -06'00'  
\_\_\_\_\_  
*Dr. Shankar Mahalingam* College Dean  
(Date)

\_\_\_\_\_  
*Dr. Jon Hakkila* Graduate Dean  
(Date)

## Abstract


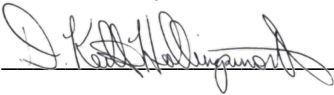
School of Graduate Studies  
The University of Alabama in Huntsville

Degree Master of Science in Engineering College/Dept. Engineering/Mechanical and  
Aerospace Engineering

Name of Candidate Timothy Daniel Robert Morris

Title EXPERIMENTAL MEASUREMENTS OF THE WING DEFORMATION AND  
FORCE PRODUCTION OF REAL MONARCH BUTTERFLY WINGS

Monarch Butterflies are capable of flying over 4000 kilometers as they migrate from North America to Mexico. In regard to the aerodynamic mechanisms that drive this extensive flight, little is known. This thesis is motivated by the hypothesis that their flapping wing flight is enhanced by fluid-structure interactions. The objective was to quantify the aeroelastic performance of a real monarch butterfly wing at flapping amplitudes near monarch free-flight amplitudes. The performance of the real monarch butterfly wing was tested by measuring the wing motion and lift at a flapping amplitude of  $55^\circ$  and frequencies between 7.0 and 14.4 Hz. The wing produced a peak lift at 10.3 Hz, approximately the flapping frequency of a live monarch butterfly, with a maximum force of 8.4 mN, sufficient to lift a butterfly's weight. The pitch amplitude increased linearly as the frequency increased with the pitch amplitude at the peak lift being  $15.8^\circ$ .

Abstract Approval: Committee Chair   
Department Chair   
Graduate Dean \_\_\_\_\_

# TABLE OF CONTENTS

|  |             |
|--|-------------|
| <b>Abstract.....</b>   | <b>iv</b>   |
| <b>Acknowledgments .....</b>   | <b>vii</b>  |
| <b>List of Figures.....</b>  | <b>viii</b> |
| <b>List of Tables .....</b>  | <b>xi</b>   |
| <b>Chapter 1. Introduction.....</b>                                    | <b>1</b>    |
| 1.1 Background and Motivation .....                                    | 1           |
| 1.2 Monarch Butterfly Migration, Aerodynamics and Wing Structure ..... | 1           |
| 1.3 Novel Contributions.....   | 3           |
| 1.4 Objective .....  | 4           |
| 1.5 Outline.....   | 5           |
| <b>Chapter 2. Literature Study.....</b>                                | <b>6</b>    |
| 2.1 Monarch Butterfly Migration.....                                   | 6           |
| 2.2 Flapping Wing Aerodynamics .....                                   | 8           |
| 2.3 Insect Wing Material Properties .....                              | 9           |
| 2.4 Butterfly Wing Angles and Force Measurements.....                  | 11          |
| <b>Chapter 3. Methodology .....</b>                                    | <b>15</b>   |
| 3.1 Wing Motion and Force Measurements.....                            | 15          |
| 3.2 Design of Experiments.....   | 20          |

|   |           |
|---|-----------|
| <b>Chapter 4. Results and Discussion.....</b> | <b>22</b> |
| 4.1 Wing Angles for a Real Wing.....          | 22        |
| 4.2 Force Generation by Real Wing .....       | 28        |
| <b>Chapter 5. Conclusion .....</b>            | <b>30</b> |
| 5.1 Conclusion .....                          | 30        |
| 5.2 Future Work.....                          | 31        |
| 5.3 Acknowledgements.....                     | 31        |
| <b>References.....</b>                        | <b>32</b> |
| <b>Appendix .....</b>                         | <b>39</b> |

To my family and friends



## List of Figures

| FIGURE   | PAGE |
|--|------|
| 2.1: Monarch Migration patterns .....  | 7    |
| 2.2: Great Flight Diagram, from Kang et al. [49]. .....  | 9    |
| 2.3: Flexural stiffness plots of sixteen different species in both the spanwise and chordwise direction. From Combes and Daniel[22].....   | 10   |
| 2.4: Representative time histories of the flapping angle, feathering angle, and deviation angle of a real monarch butterfly wing mounted on the gearbox and operated at an input voltage of 1.1 V.. .....        | 12   |
| 2.5: Representative time histories of the flapping angle, feathering angle, and deviation angle of an artificial monarch butterfly wing mounted on the gearbox and operated at an input voltage of 1.1 V.. ..... | 13   |
| 2.6: Lift forces produced by real and artificial wings during the Micron flapper experiments at different flapping frequencies.. .....   | 14   |
| 3.1: An ATI Nano force transducer mounted on a custom 3D printed base, with a foam layer inserted between the upper and lower halves of the mount to act as a vibration dampener. ....                           | 16   |
| 3.2: The flapper gearbox and wing mounted to the right side. ....  | 18   |
| 3.3: Z-component of the LE marker per frame for one and a half cycles at a sampling rate of a) 200 Hz and b) 400. ....   | 18   |
| 3.4: VICON system setup to record the deflections of a wing attached to a gearbox.. ....   | 19   |

|   |    |
|---|----|
| 4.1: Representative time histories of the flapping angle, feathering angle, and deviation angle of a real monarch butterfly wing mounted on the gearbox and operated at an input voltage of 0.7 V. .... | 23 |
| 4.2: Representative time histories of the flapping angle, feathering angle, and deviation angle of a real monarch butterfly wing mounted on the gearbox and operated at an input voltage of 1.1 V. .... | 25 |
| 4.3: The mean feathering angle for 20° (red) and 55° (blue) flapping amplitudes versus frequency. ....  | 26 |
| 4.4: Lift forces produced by a monarch wing at 20° and 55° flapping amplitudes for a range of different flapping frequencies.....   | 29 |
|   |    |
| A.1: Representative time histories of the flapping angle, feathering angle, and deviation angle of a real monarch butterfly wing mounted on the gearbox and operated at an input voltage of 0.5 V.....  | 38 |
| A.2.: Representative time histories of the flapping angle, feathering angle, and deviation angle of a real monarch butterfly wing mounted on the gearbox and operated at an input voltage of 0.6 V..... | 39 |
| A.3.: Representative time histories of the flapping angle, feathering angle, and deviation angle of a real monarch butterfly wing mounted on the gearbox and operated at an input voltage of 0.8 V..... | 40 |
| A.4: Representative time histories of the flapping angle, feathering angle, and deviation angle of a real monarch butterfly wing mounted on the gearbox and operated at an input voltage of 0.9 V.....  | 41 |

A.5: Representative time histories of the flapping angle, feathering angle, and deviation angle of a real monarch butterfly wing mounted on the gearbox and operated at an input voltage of 1.0 V..... 42

## List of Tables

| TABLE   | PAGE |
|---|------|
| 3.1: Input Voltages.....  | 20   |
| 4.1: Morphological data for a real monarch wing.....  | 22   |
| 4.2: Input voltage and corresponding flapping frequency. ....   | 24   |
| 4.3: Average phase offset of each peak for a given input voltage and corresponding<br>frequency. .... | 27   |

# **Chapter 1. Introduction**

## **1.1 Background and Motivation**

Despite visually appearing structurally the same, the monarch butterfly is unique amongst all the species of the Nymphalidae family in its ability to travel vast distances, up to 4000 kilometers, and is easily the one of the most recognizable butterfly species in North America [1]. During its migration, it is presumed that monarchs use the low atmospheric density at high altitudes to their advantage to aid in soaring flight and reduce aerodynamic drag [2]. However, the detailed aerodynamic phenomena driving the three-month journey is yet unknown.

The wings of the monarch are flexible structures, allowing them to deform significantly during flight. This is significant as flexible flapping wings are capable of generating large forces with considerably less power consumption when compared to their rigid counterparts [3–19]. Monarch wings exhibit an anisotropic nature in that their spanwise flexibility differs from that of their chordwise flexibility [5,20,21] and likewise, the dorsal flexibility from the ventral [22–24]. This anisotropic nature is in large part due to the membrane and vein structure in the wing and one-way hinges that use resilin [25].

## **1.2 Monarch Butterfly Migration, Aerodynamics and Wing Structure**

Annually, the monarch butterfly ventures thousands of kilometers to a never before visited winter camp, relying on food stops along the way, in the mountains of central

Mexico [26–29]. There, they wait out their diapause before returning north for the summer [26,27,30,31]. Their migration is one of the more extraordinary natural phenomena amongst the butterfly species that exist in North America. Despite the hundreds of thousands that make the journey to Central Mexico, they all end their journey in the same location, which was not discovered until 1975 [32]. The overwintering camp in itself is also impressive as it requires ample food and water sources to feed hundreds of thousands of monarchs. It also must have shaded and sunny regions for thermoregulation, protection from wind gust, and the correct types of trees [33,34]. As such a habitat is complicated and rare, it is important to preserve them and to study and gather as much information of the monarch's unique species characteristics, navigational skills, and flight capabilities.

For years, the flight dynamics of insects has been of interest. In particular, they have been a source of inspiration and information for the development of micro flying robots, the study of low-Reynolds number vortex dynamics [7,9,13,17,18,20,35], and quantifying the efficiency of flexible wings [4,5,8–11,15,36]. Insects are capable of incredible maneuvering and lift generation as small, lightweight , streamlined organisms and having wing structures with high surface area. They are capable of stable flight aided by the coupling of their body undulation and wing flapping [13,15,20], which contributes to their energy preservation and thus the overall efficiency during their migrations [37]. It is implied that the material properties of the wing may impact flight efficiency as the fluid surrounding a deforming flapping wing is altered.

Research on the material properties of insect wings, in addition to their aerodynamics, can provide insight into their performance capabilities. The characteristics of a material dictate how a structure will interact with its surroundings or react to forces

and are therefore, important to study. Material properties such as flexural stiffness and density for insect wings have previously been researched [22–24,38–40]. Combes and Daniel [22], Steppan [24], and Tanaka and Wood [23] found that the flexibility in insect wings when measured along the chordwise versus the spanwise direction differed as well as if the wing was dry versus wet [22,24]. Wainwright [39], Jensen and Weis-Fogh [40], and Song et al. [38] measured the densities of different insect wings. However, the monarch butterfly was not included amongst the species research. As monarchs are the only species in North America to migrate great distances, their flight capabilities are of particular interest.

Aerodynamic and viscoelastic damping can also dictate a structures response [41,42]. However, modeling and analyzing these effects can be difficult as this constitutes a closely coupled dynamical system [42]. The study of the wing motion and force generation of a monarch will aid in future model developments.

### **1.3 Novel Contributions**

Improvements have been made to the experimental setup seen in previous work [43]. An in-house flapper was designed and produced to provide flapping amplitudes closer to the flapping amplitude of a monarch butterfly in free flight. To capture the higher amplitude motion of the wing additional VICON cameras were installed and the VICON equipment was increased to 400 Hz, doubling the data sampling rate. Furthermore, the experimental setup was run completely by one operator. Post-processing of the recorded data was also improved greatly.

## 1.4 Objective

In this study, the working hypothesis is that the fluid-structure interaction between the monarch wings and the surrounding unsteady flow produces sufficient lift while reducing the power consumption. It is theorized that this reduction in power consumption makes possible the long-range migrations seen in monarchs and is due to the coupled wing-body dynamics, and the presumed aerodynamic efficiency given by the fluid-structure interaction of large flexible wings. It is these mechanisms that can help develop butterfly-inspired micro-air vehicles (MAVs) that are capable of long-range flight missions. However, literature lacks any sufficient studies on the aerodynamic forces produced by a wing flapping at large amplitudes.

The goal of this thesis is to quantify the aeroelastic performance of monarch butterfly wings at large flapping amplitudes. To accomplish this, the force and deformation created by a real monarch butterfly wing was simultaneously measured using an ATI Nano force transducer and a VICON motion capture system respectively. The results were then compared to those of the real monarch wing flapping at lower flapping amplitudes and tested under similar conditions in a study done by Twigg [43]. Although Monarch flights showcase noticeable vertical undulations and body pitch, this study focuses on the relations between the resulting aerodynamic forces and wing deformations while keeping the body fixed. Nevertheless, the information obtained will support further development of bioinspired long-range micro-air vehicles, which, in turn, supplements our knowledge of how these insects are capable of such an impressive migration.



## 1.5 Outline

A literature study is presented in Section 2, detailing monarch migration (Section 2.1), flapping aerodynamics (Section 2.2), insect wing material properties (Section 2.3), and a recent study on the wing angles and force generation of a monarch wing at a  $20^\circ$  flapping amplitude (Section 2.4). The experimental methodology is described in Section 3, covering the wing motion measurements (Section 3.1), force measurements (Section 3.2), and the design of experiments (Section 3.3). Then, the results are discussed in Section 4. This includes wing angles for a real wing (Section 4.1), and force generation by a real wing (Section 4.2). Finally, a conclusion is given in Section 5, providing concluding remarks (Section 5.1), the direction of future work (section 5.2), and lastly acknowledgments (5.3).

## **Chapter 2. Literature Study**

A comprehensive and recent literature study was presented in Twigg [43]. A summary of the literature and work done is presented in this chapter.

### **2.1 Monarch Butterfly Migration**

Monarchs vary from other butterfly species and within their own genus. They can be found in three different and distinct locations in North America [44]. Their migration patterns are one example of how they vary. Monarchs found solely in Florida migrate relatively short distances along the southeastern coast of the United States of America [44,45], whereas populations found on the west side of the Rocky Mountains migrate to northwestern areas of North America in the summers and then along the coast of California in the winter. Both have a much less migration distance than their counterparts found on the east side of the Rocky Mountains, who migrate distances up to 4000 km from their summer residences in parts of Canada to their overwintering sites in Central Mexico [26,27,30] (Figure 2.1). Further differences include their colorations, where Eastern populations tend to exhibit darker wings with large black regions and western populations having brighter wings with more orange [44,46]. Their muscle regions also vary, which indicates that they may contribute to the ability to travel long distances [47].



**Figure 2.1: Monarch Migration patterns.**

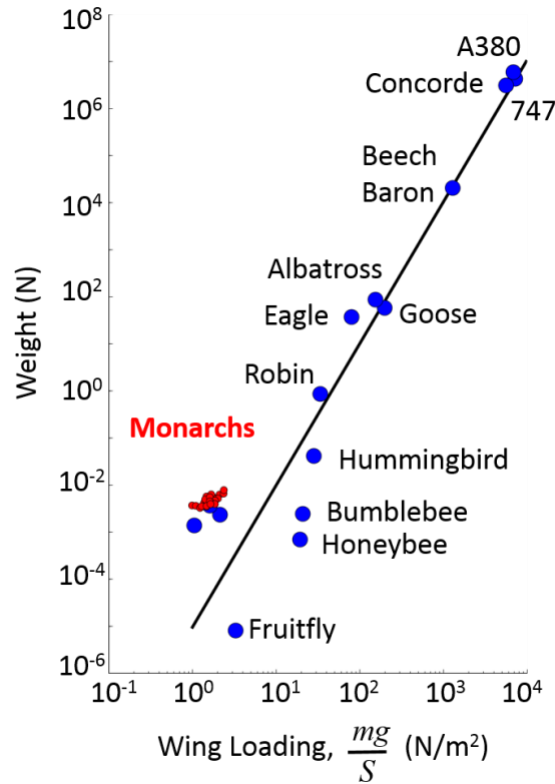
Over the 4000 km migration, monarchs are able to cover up to 50 km in a day through use of a combination of gliding, soaring, and powered flight [26,27,48,49]. Brower [26] and Gibo [48] show that monarchs take advantage of thermals to gain altitude, and either continue to soar the altitudes gained, or glide continuously until powered flight is needed. This variation of flight modes can contribute to energy conservation [50] and enhance their flight speeds by utilizing the fast tail winds present in the upper altitudes. In the case of unfavorable weather or wind conditions, such as storms or head winds, monarchs either waited until conditions were more desirable or utilized powered flight at lower altitudes where less power is required to resist head winds or wind gust as air velocities closer to the ground are much lower compared to the altitudes that monarchs are capable of achieving [26,27,48,49].

## 2.2 Flapping Wing Aerodynamics

Butterflies benefit, in part, from unsteady aerodynamic mechanisms such as leading-edge vortex generation and shedding, wake-capture, and clap and fling [1,3]. However, their flight has been understudied due to the closely coupled wing-body dynamics and the fluid structure interaction of their large, thin wings, flapping at a relatively low frequency.

The Monarch butterfly has the lowest wing loading (Figure 2.2) compared to other insects [22], despite their large wings relative to their thin body. This leads to the monarch's unique agility [4,12–14]. Their body undulations are linked with the motion of their wings [13,15], which possibly aids in their pitch stability during forward flight [20]. Such a wing-body coupling potentially aids in their long-range migration due to the reduction in power consumption [37].

Insect wings contain fluid-structure mechanisms that can aid in reducing drag and increase lift, however, there are no studies involving these mechanisms with monarchs to-date. Thrust increases are caused by vortices generated along the wing surface and shed in the downstream direction, creating a reverse von Karman street [9,13]. Insects do not possess the muscle ability to pitch their wings and rely on passive pitching which allows the leading-edge vortices to stay attached to the surface for longer, leading to an overall increase in lift production [7,8,20].



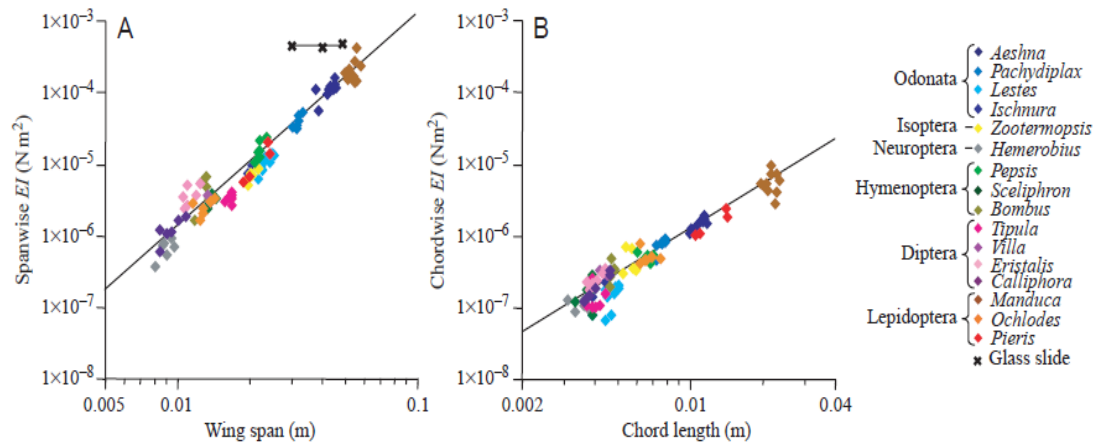
**Figure 2.2: Great Flight Diagram, from Kang et al. [49]. Reprinted by permission.**

Wing flexibility allows for the minimization of disturbances during wind gusting [11], and asymmetric bending which is indicative of anisotropic characteristics. This leads to the wing producing different levels of lift on the upstroke versus the downstroke [15]. It has been surmised that there exists an optimum wing flexibility that produces the greatest lift in correlation with efficiency [4,5,8,19]. However, the detailed fluid-structure interaction mechanism is inadequately understood.

### 2.3 Insect Wing Material Properties

Wing anisotropy has been studied for a multitude of different insect species [22–24,35,51,52]. Combes and Daniel [22] performed an extensive study, measuring and recording both the spanwise and chordwise stiffness for sixteen different species (Figure 2.3). They concluded that the spanwise stiffness was one or two orders of magnitude

greater than the chordwise stiffness. Steppan [24] also demonstrated this in his experiment and further showed that the stiffness of the wing increased as it dried, driving the urgency to gather data while the wing is fresh. Twigg et al [43] proved similar results in her experiment and with the aid of a Micro-CT scanner, was able to manufacture an artificial butterfly wing, discuss further in section 2.4.



**Figure 2.3: Flexural stiffness plots of sixteen different species in both the spanwise and chordwise direction. From Combes and Daniel[22]. Reprinted by permission.**

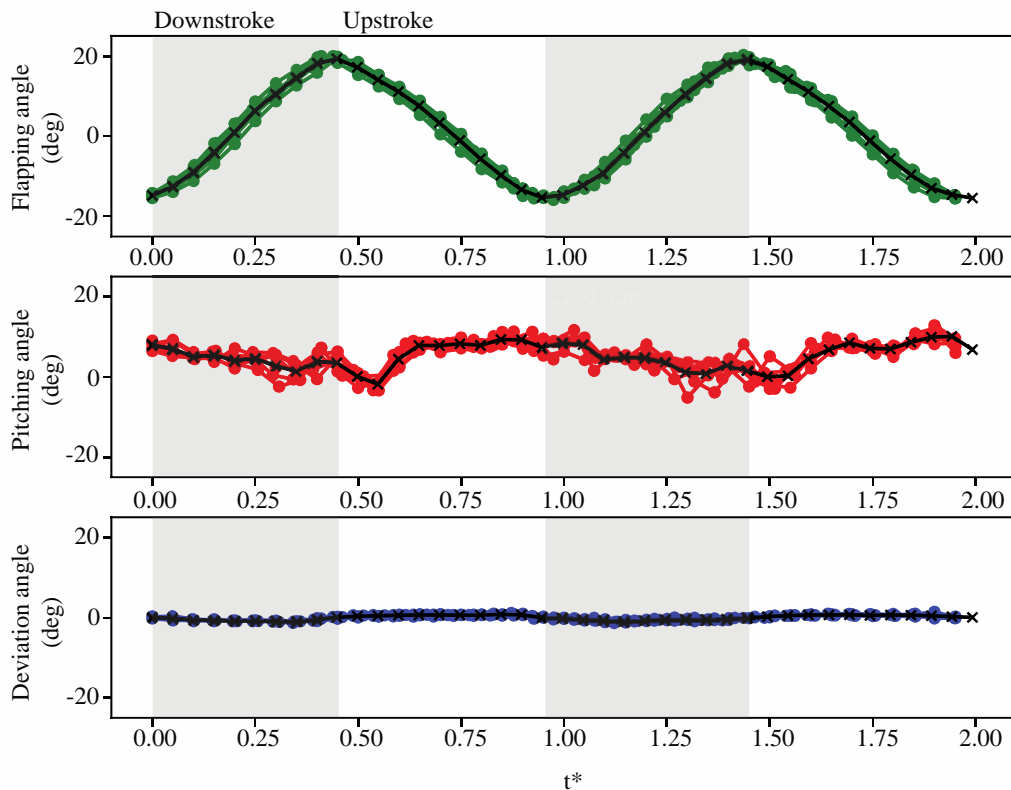
To facilitate the manufacturing of a detailed artificial butterfly wing, Twigg first determined the density and wing structure of a Monarch butterfly wing [43]. A micro-CT scan provided the wing image information at a spatial resolution of 10  $\mu\text{m}$ . With the data provided by the micro-CT scan, the volume of the wing was determined. With this volume and the weight of the wing, which was measured before the CT scan, the density of the wing was found to be 307  $\text{kg}/\text{m}^3$ . This value differs greatly from other studies, mostly of which cite Wainwright et al [39] in which a density value of 1200  $\text{kg}/\text{m}^3$  is reported. However, the difference in the two values is likely explained by the difference in species that each tested. Twigg’s value was determined for a Monarch butterfly (D.

plexippus) and Wainwright's was determined for a blowfly (*Phormia*). Furthermore, Twigg's method involved sophisticated equipment unavailable to Wainwright, which gave a much more accurate model a butterfly wing.

## **2.4 Butterfly Wing Angles and Force Measurements**

The motion of a flapping butterfly wing is not very well understood. In a recent study by Twigg [43], an experiment was performed to determine the motion of the wing and how much lift it could produce. A Micron [53] 6mm Ornithopter gearbox was mounted to an ATI Nano 17 Titanium force transducer to simultaneously measure the wing motion and the wing forces. Three reflective markers were placed on a fresh Monarch wing and two more on the longitudinal axis of the gearbox. Six VICON T40 motion capture cameras were placed around the butterfly wing and used to record the three-dimensional positions of the markers while the wing was flapping. Both the VICON cameras and force transducer recorded at a sampling rate of 200 Hz for 5 s and were triggered simultaneously such that their time histories were correlated.

Using this method, a series of tests were performed. Each test had a different flapping frequency depending on the input voltage to the flapper and was repeated six times. Figure 2.4 demonstrates the wing angles for a real monarch wing mounted on the gearbox and operated at an input voltage of 1.1V. The corresponding average frequency for this test was 10.3 Hz, which is approximately the flapping frequency of a monarch butterfly in free flight [54].



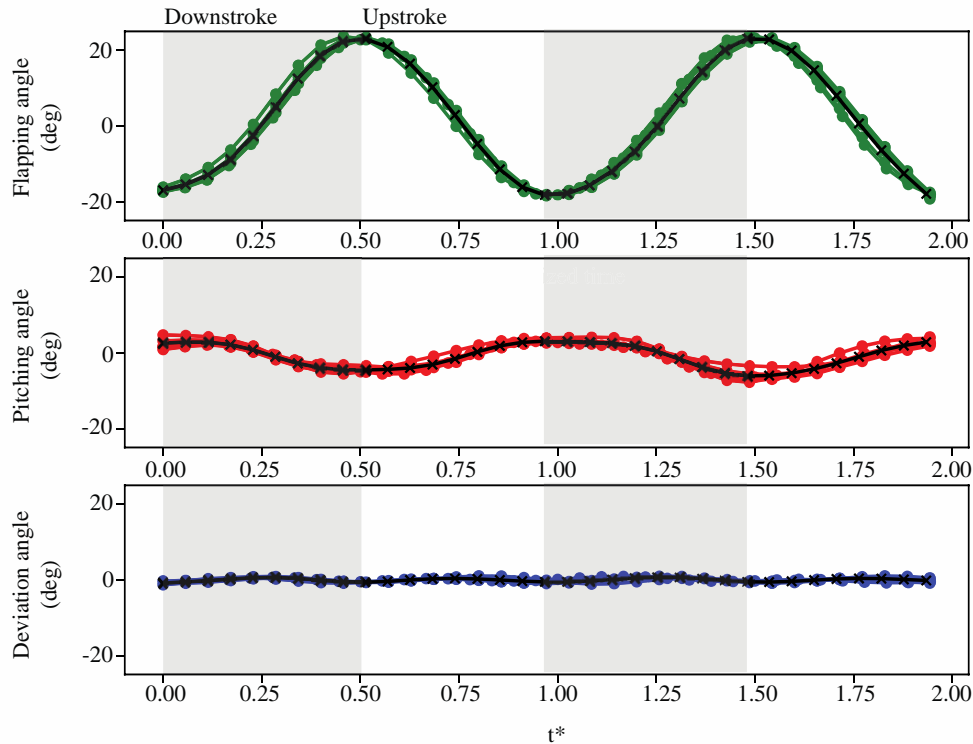
**Figure 2.4: Representative time histories of the flapping angle, feathering angle, and deviation angle of a real monarch butterfly wing mounted on the gearbox and operated at an input voltage of 1.1 V. The FFT analysis of the flapping motion indicates that the flapping frequency was 10.3 Hz. The grey bars indicate the downstroke, and the white bars indicate the upstroke. The black line is the average of each subplot (n=6). Reprinted by permission [43].**

Though a small variation in flapping angle was present amongst the six tests, the average flapping angle was approximately  $20^\circ$ , which is the amplitude of the gearbox. However, this flapping angle is considerably less than the flapping angle of a monarch in free flight,  $64^\circ$ . The tests also showed that the feathering angle was approximately sinusoidal with a phase lag of  $155^\circ$ - $190^\circ$ . This means that the wing's pitching motion is a half-stroke behind the flapping motion.

Twigg also performed the same test on an artificial wing. The vein structure of the wing was three-dimensionally printed using the three-dimension model generated from a micro-CT scan of a real monarch butterfly wing (section 2.3). The vein structure was then



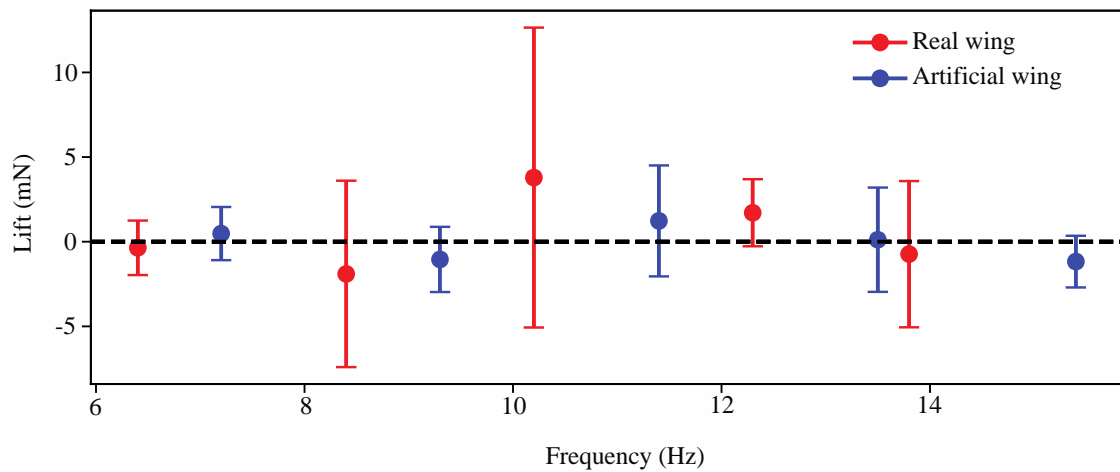
chemically bonded to a sheet of PLLA, which emulated the membrane of the real wing. The results showed a remarkably similar trend in wing motion. However, there was a noticeable difference in the wings flapping frequency given the same input voltage of 1.1V. This difference was thought to be due to the difference in the thickness of the veins and the density of the wing material. Figure 2.5 demonstrates the wing angles for an artificial butterfly wing with an input voltage of 1.1V, corresponding to an average frequency of 11.4 Hz,



**Figure 2.5: Representative time histories of the flapping angle, feathering angle, and deviation angle of an artificial monarch butterfly wing mounted on the gearbox and operated at an input voltage of 1.1 V. The FFT analysis of the flapping motion indicates that the flapping frequency is 11.4 Hz. The grey bars indicate the downstroke, and the white bars indicate the upstroke. The black line is the average of each subplot (n=6). Reprinted by permission [43].**

Figure 2.6 represents the resulting lift forces for both the real and artificial wing. The max force produced by the real wing is 3.8 mN. As this force is produced by only one wing, it is believed that even at this relatively small flapping amplitude that the butterfly

would have sufficient lift to overcome both its weight of approximately 5 mN (75) and any external forces it may encounter during flight. The artificial wing's peak force, however, was only 1.3 mN. It was theorized that this was due to the PLLA membrane being homogenous whereas the real butterfly wing had an anisotropic membrane. Another factor that may have contributed to the lower lift generation is the difference in vein structure. The artificial wing was manufactured with a uniform rectangular non-hollow vein structure whereas the real wing possesses a circular tapered hollowed vein structure.



**Figure 2.6: Lift forces produced by real and artificial wings during the Micron flapper experiments at different flapping frequencies. The error bars represent the 95% confidence interval (n=6). Reprinted by permission.**

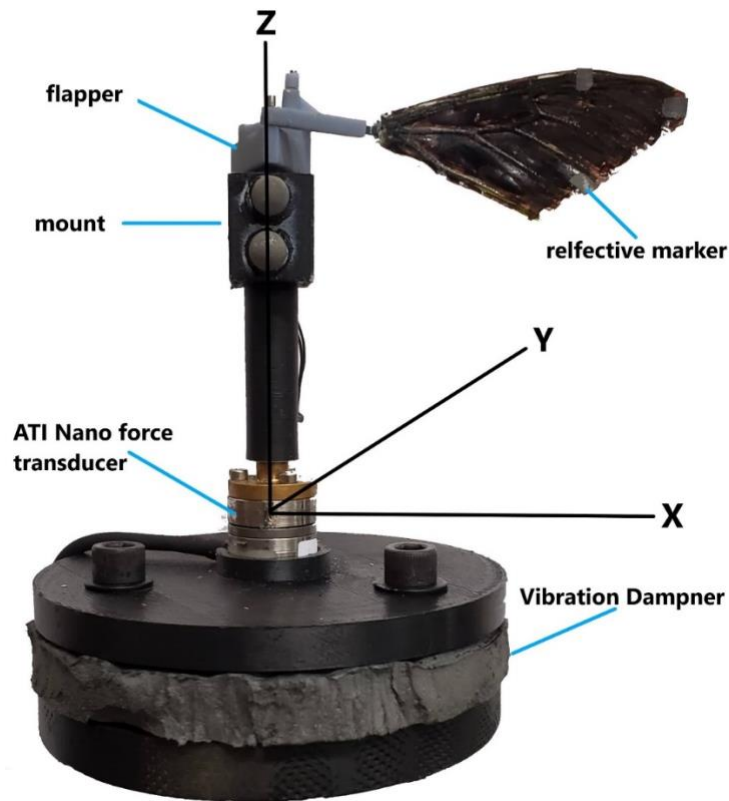
## **Chapter 3. Methodology**

The goal of this study is to quantify the wing motion and force generation of monarch butterfly wings at flapping amplitudes near monarch free-flight amplitudes. The wing motion of a real monarch butterfly wing was measured at different frequencies ( $f$ ) (Section 3.1). The gearbox prescribed a fixed amplitude flapping wing motion. In a monarch butterfly flight, the flapping angle changes as the wing passes through different parts of the stroke, while the feathering angle passively changes. The force generation was simultaneously measured (Section 3.2), allowing for the lift ( $L$ ) generation to be characterized.

### **3.1 Wing Motion and Force Measurements**

The experimental setup for the deformation and force measurements of the real butterfly wing comprised of a set of VICON T40s motion capture cameras and an ATI Nano 17 Titanium force transducer. An in-house three-dimensional printed mount was used to attach the flapper to the ATI Nano force transducer such that the lift direction of the flapper was aligned with the  $+z$ -axis of the force transducer (Figure 3.1). This orientation was chosen to maximize the power output from the motor to the flapper, as the flapper does not have to flap against gravity, potentially allowing more accurate and consistent results. To capture the higher amplitudes associated with a monarch's free flight, the test stand was surrounded by VICON T40 cameras. To prevent interference with VICONs ability to capture the wing motion, reflective surfaces on and around the test setup

up were painted black and black paper was used to provide a dark non-reflective background.

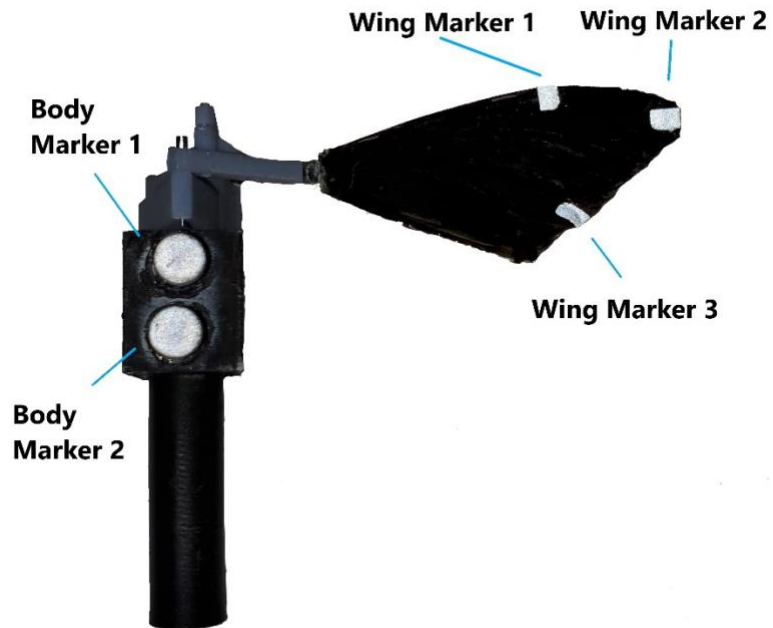


**Figure 3.1: An ATI Nano force transducer mounted on a custom 3D printed base, with a foam layer inserted between the upper and lower halves of the mount to act as a vibration dampener. The in-house three-dimensionally printed flapper was attached using a custom three-dimensionally printed mount. The wing was attached to the flapper with a carbon fiber rod glued to the root of the wing. The flapper flaps with a peak-to-peak amplitude of  $120^\circ$  in the x-y plane such that the lift produced by the wing is in the +Z axis.**

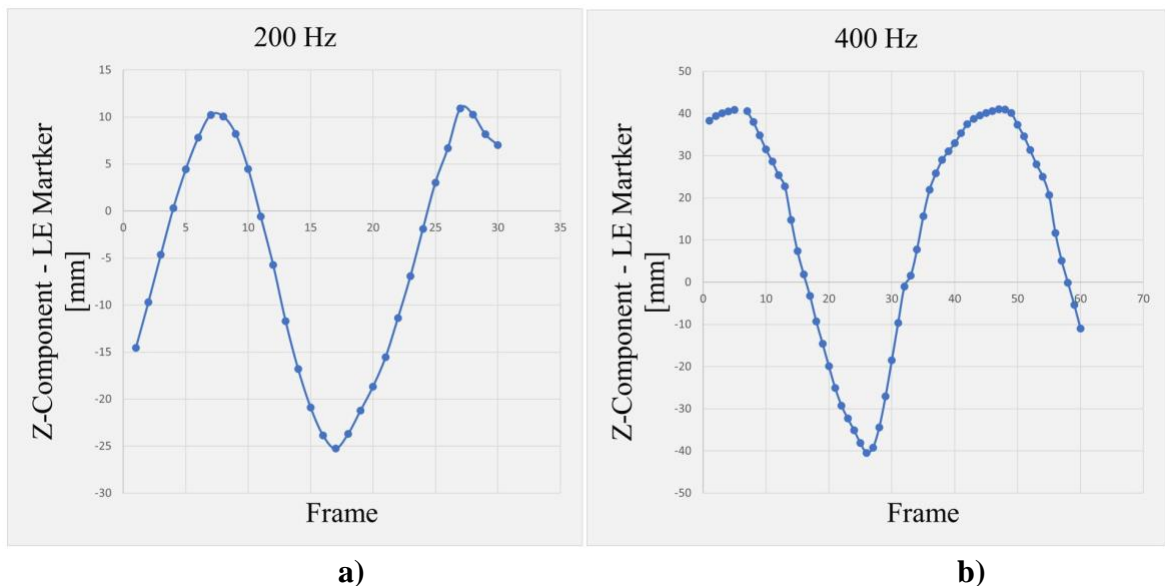
Three small reflective surfaces were placed on the wing and two reference markers on the longitudinal axis of the body (Figure 3.2). Each marker was  $6 \times 2.34$  mm in size and their combined mass was approximately 1.7% the mass of the butterfly and 42.8% the mass of the wing. The three-dimensional positions of the markers were captured using the same

optical measuring techniques to measure the three-dimensional wing kinematics of a real butterfly in climbing flight [54]. However, a sampling rate of 400 Hz was used for a duration of 2 sec. This sampling rate was a significant improvement over the 100-200 Hz used in previous studies and was the result of reducing the noise by ensuring there is no reflective surfaces within the VICON camera's field of view [43,54]. Furthermore, an increased sampling rate provided a higher number of data points per cycle (Figure 3.3), reducing any data gaps caused by VICON being unable to identify a marker. Missing data markers were interpolated using a cubic-spline interpolation [54].

The force generated by the butterfly wing motion was recorded by the force transducer at a sampling rate of 1000 Hz for 2 sec. Before the experiment was ran, the load due to the butterfly wing's weight was zeroed. The VICON camera recording, and the force transducer recording were simultaneously triggered such that the time histories of the wing motion and force were correlated. We previously used the same techniques to simultaneously measure the three-dimensional wing kinematics and forces of a real and artificial wing flapping at a peak-to-peak flapping amplitude of 40 deg [43].

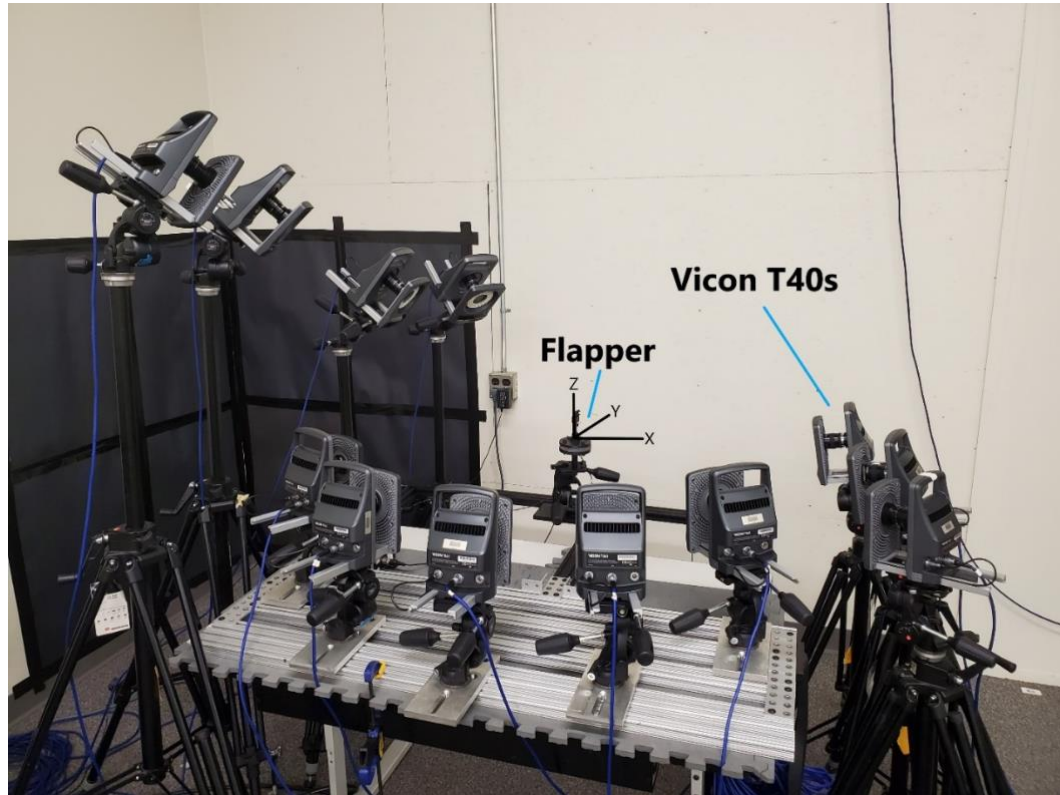


**Figure 3.2:** The flapper gearbox and wing mounted to the right side. Three wing markers forming a triangle in addition to two body markers were used to calculate Euler angles.



**Figure 3.3:** Z-component of the LE marker per frame for one and a half cycles at a sampling rate of a) 200 Hz and b) 400. More data points per cycle provides a clearer picture and reduces the data gap caused by missing data points.

The equipment for the real wing experiments consisted of twelve VICON cameras that encircled the wing from different angles and heights to ensure full coverage of the wing motion. The body and wing markers were placed as seen in Figure 3.4, with the primary wing marker placed on the front of the in-house mount and the secondary body marker placed 10mm in the -z direction.



**Figure 3.4: VICON system setup to record the deflections of a wing attached to a gearbox. The wing was attached to a force transducer which simultaneously recorded the forces produced during the flapping. The gearbox is oriented with the lift direction along the +z-axis.**

The flapping, feathering, and deviations angles of the real butterfly wing were determined using the position of the wing markers on the right wing and two body markers placed on the mount [43]. The flapping frequency was obtained by taking the Fast-Fourier transform (FFT) of the time history of the flapping angle. The force transducer output was

connected to a National Instruments DAQ, and the measured data was saved to an external computer. The wing motion data was smoothed using a low pass filter with a cut off frequency of 30 Hz, which is three times the flapping frequency of a monarch in free flight [43]. The recorded force data, which included higher frequency oscillations, were also filtered using a low pass filter with a cut off frequency of 30 Hz.

### 3.2 Design of Experiments

The real wing was tested at a series of input voltages which were directly correlated to frequency. From studies done at 20° flapping amplitudes [43], it was found that a real monarch butterfly wing required an input voltage of 1.1 V to achieve a frequency of approximately 10 Hz, which is the flapping frequency of a monarch in free flight [54]. Given the large increase in flapping amplitude and changes made to the experimental set-up, the wing was initially tested at the lowest possible input voltage the flapper would operate at, 0.5 V, and then increased by 0.1 V increments until there was failure in the wing, 1.1 V (Table 3.1). For repeatability, four tests were performed at each voltage.

**Table 3.1: Input Voltages**

|               |     |     |     |     |     |     |                  |
|---------------|-----|-----|-----|-----|-----|-----|------------------|
| Input Voltage | 0.5 | 0.6 | 0.7 | 0.8 | 0.9 | 1.0 | 1.1<br>(failure) |
|---------------|-----|-----|-----|-----|-----|-----|------------------|

The data collected for each test using the VICON cameras was processed using VICON NEXUS and exported to an ANSCII file. The exported data included the time histories of the three-dimensional positions of each of the three wing markers and the two



body markers. This data was then further processed using a PYTHON script, which provided the wing angles and corresponding flapping frequency [55].

The force data for each test was collected using the NANO 17 F/T was directly saved as a .CSV file using the program ATIDAQFT. Each data set consisted of a time history of the three-dimensional force components. This data was then process through a PYTHON script, which outputted the average force of each component and the total force magnitude.

## Chapter 4. Results and Discussion

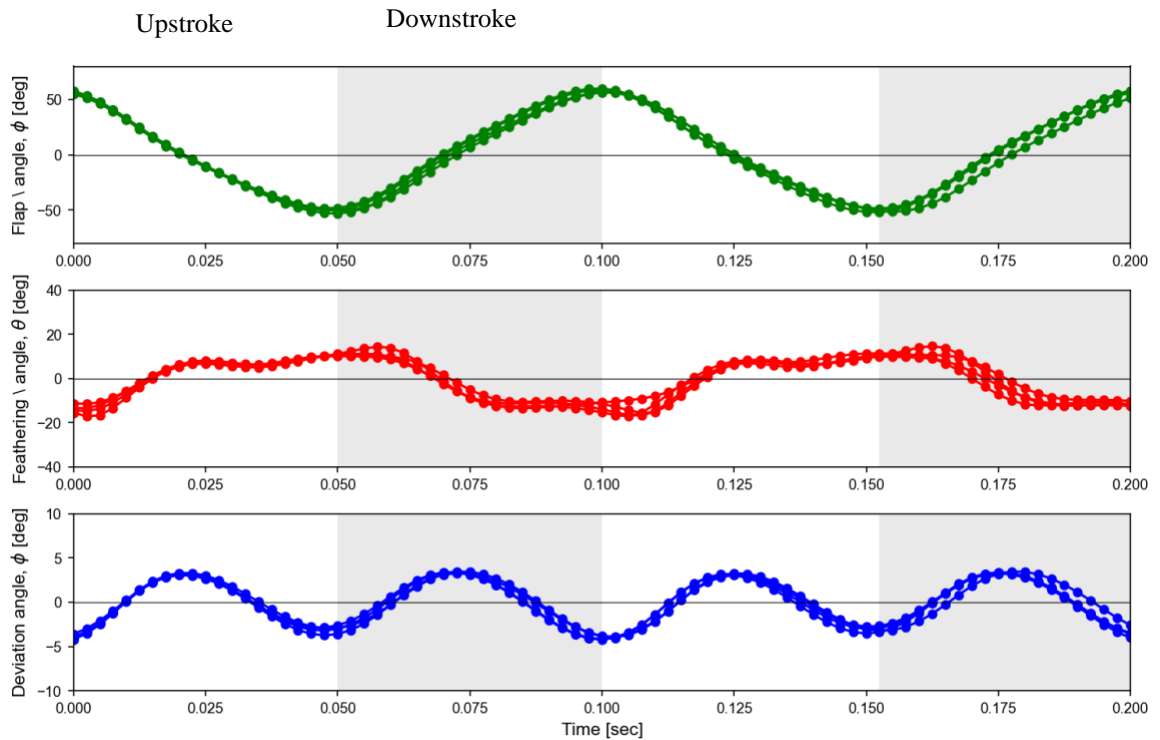
### 4.1 Wing Angles for a Real Wing

Table 4.1 displays the morphological data for the wing. Figure 4.1 illustrates the wing angles for a real monarch wing flapping at approximately 10.3 Hz and 55°. The frequency and amplitude of a monarch in free flight is 10 Hz and 64°, respectively. Both the flapping and feathering angles have minimal variation between the four repeated measurements demonstrating a consistency in the performance of both the gearbox and wing. The deviation angle is larger than the deviation of a wing flapping at a similar frequency but at a flapping amplitude of 20°, but still remains small enough to indicate that

**Table 4.1: Morphological data for a real monarch wing**

| Wing mass<br>(g) | Span<br>( $\times 10^{-3}$ m) | Chord<br>( $\times 10^{-3}$ m) | Area<br>( $\times 10^{-4}$ m <sup>2</sup> ) | Wing side |
|------------------|-------------------------------|--------------------------------|---|-----------|
| 0.0194           | 53.111                        | 27.307                         | 942.061                                     | Right     |

the wing did not have any unanticipated movements.



**Figure 4.1: Representative time histories of the flapping angle, feathering angle, and deviation angle of a real monarch butterfly wing mounted on the gearbox and operated at an input voltage of 0.7 V. The FFT analysis of the flapping motion indicates that the flapping frequency was 10.3 Hz. The grey bars indicate the downstroke, and the white bars indicate the upstroke. \*The original data was shifted to be symmetric about the x-axis.**

The flapping frequency was obtained by taking the Fast-Fourier transform (FFT) of the time history of the flapping angle. Table 4.2 presents the average flapping frequency and its corresponding voltage for both 20° and 55° flapping amplitudes. The flapping amplitude was defined as half of the difference between the maximum and minimum flapping angle.

At an average flapping amplitude of 55 deg, an input of 0.7 V was required to give an average flapping frequency of 10.3 Hz. The average flapping amplitude is the mean of the flapping amplitudes from all the trials. Comparatively, when the average flapping amplitude was lower at 20 deg, it was found that an input voltage of 1.1 volts was required to achieve a similar average flapping frequency of 10.2 Hz [43]. This is likely due to the difference in motor used to perform the experiment. A more efficient motor was used and

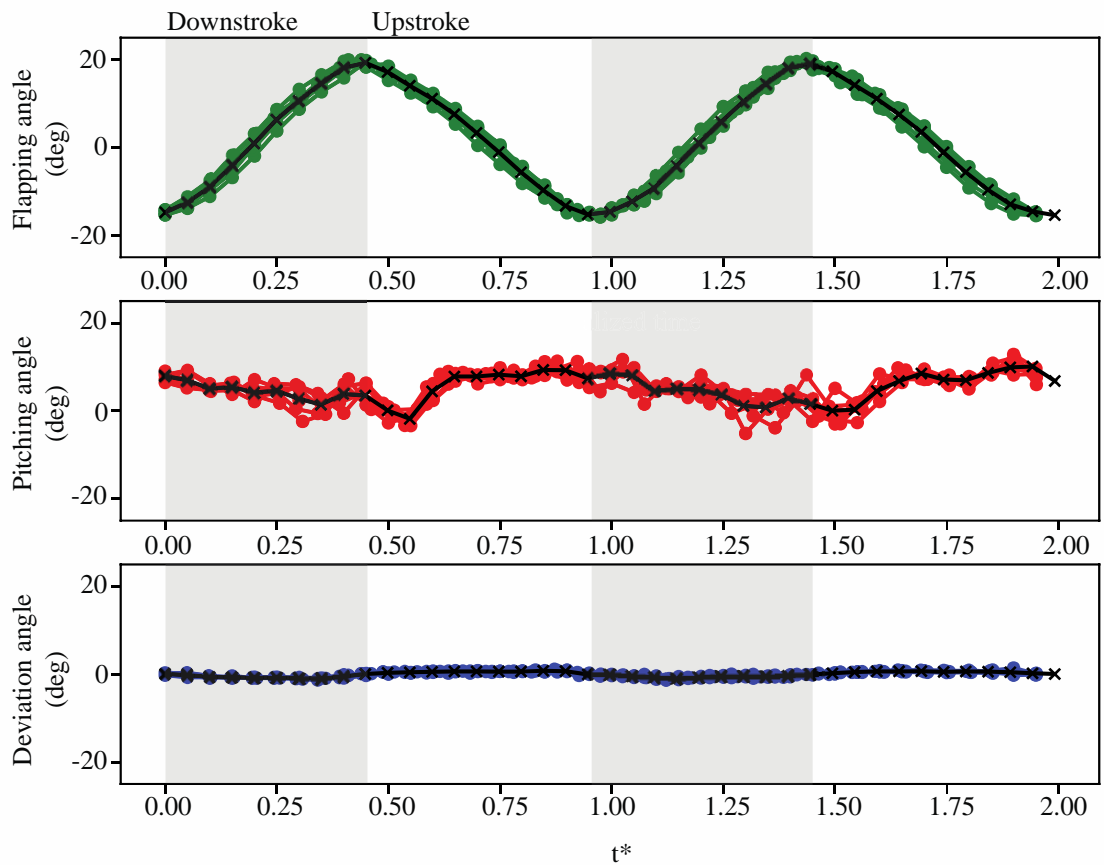
therefore required less power input to achieve higher flapping frequencies, despite the large increase in flapping amplitude.

**Table 4.2: Input voltage and corresponding flapping frequency for 20° and 55° flapping angles.**

| Input [V] | Frequency [Hz] |      |
|-----------|----------------|------|
|           | 20°            | 55°  |
| 0.5       | -              | 7.0  |
| 0.6       | -              | 8.6  |
| 0.7       | 6.4            | 10.3 |
| 0.8       | -              | 11.7 |
| 0.9       | 8.4            | 12.7 |
| 1         | -              | 14.4 |
| 1.1       | 10.3           | -    |
| 1.2       | -              | -    |
| 1.3       | 12.3           | -    |
| 1.4       | -              | -    |
| 1.5       | 13.8           | -    |

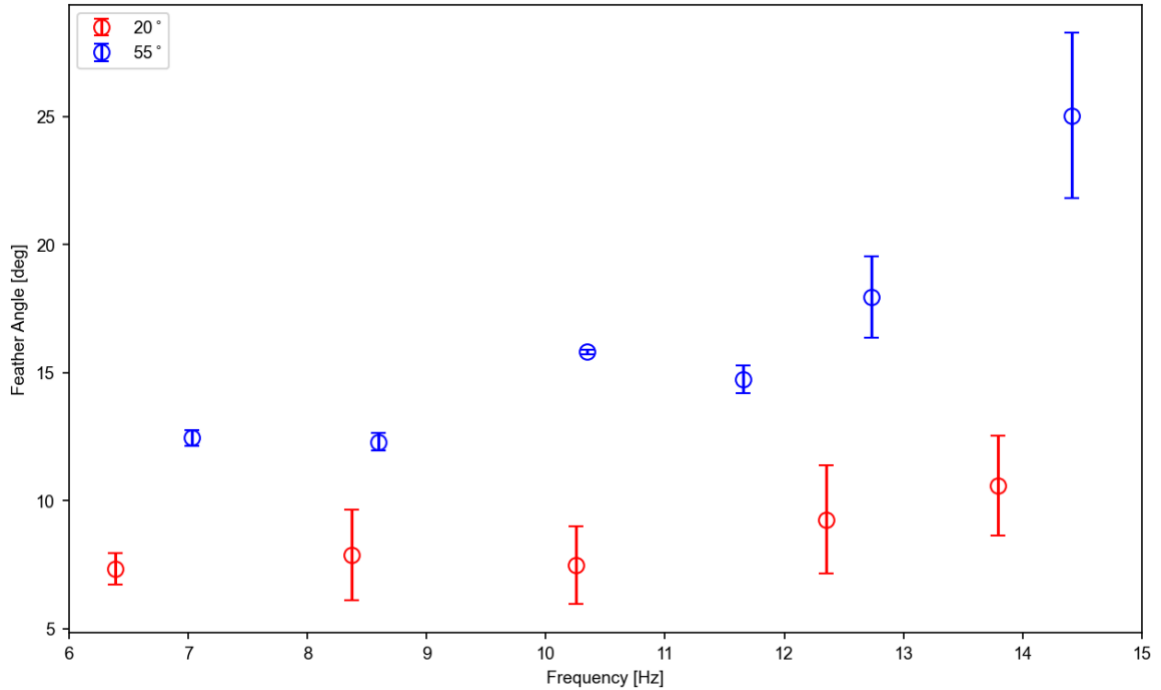
Test performed on the monarch wing at above and below the monarch’s free flight flapping frequency, 10 Hz, showed little to no effect on the average flapping angle, which is similar to the trend seen on test done at 20° flapping amplitudes [43]. This shows that the flapper was consistent in outputting the desired flapping angle of 50°-60°.

The feathering angle for 55° flapping amplitudes (Figure 4.1) differs greatly from those seen at 20° flapping amplitudes (Figure 4.2) [43]. At 20° flapping amplitudes, the feathering angle, though somewhat sinusoidal, had no clear indication of where the feathering angle peaked or its corresponding amplitude. The work of this paper shows that at higher amplitudes, the wing motion becomes much clearer and more pronounced.



**Figure 4.2:** Representative time histories of the flapping angle, feathering angle, and deviation angle of a real monarch butterfly wing mounted on the gearbox and operated at an input voltage of 1.1 V. The FFT analysis of the flapping motion indicates that the flapping frequency was 10.3 Hz. The grey bars indicate the downstroke, and the white bars indicate the upstroke. The black line is the average of each subplot (n=6). Reprinted by permission.

The average peak feathering angle increases somewhat linearly as a function of frequency, showing that the faster the wing flaps, the more it passively deforms. This trend is similar to the average peak feathering angle at 20° flapping amplitudes; however, both the overall magnitudes and rate of increase are greater at 55° flapping amplitudes (Figure 4.3). The peak lift average feather amplitude for 20° and 55° flapping amplitudes is 7.5° and 15.4°, respectively, and occurs at approximately 10.3 Hz for both.



**Figure 4.3: The mean feathering angle for 20° (red) and 55° (blue) flapping amplitudes versus frequency. The error bars represent the 95% confidence interval (nred=6, nblue=4).**

As Figure 4.1 shows, the feathering angle for a monarch wing flapping at a 55° amplitude is sinusoidal with distinct peaks. However, depending on the frequency, the feathering angle curve is a higher order harmonic than the flapping angle which is a first order harmonic. It is theorized that as the frequencies increases, the fluid-structure interaction becomes more prominent and drives the passive pitching of the wing. At lower frequencies, less than 9 Hz, the feathering angle has three peaks. As the frequency increases the number of peaks decreases with there being only one peak at frequencies near 14 Hz. Of particular note, the prominent peak occurs at the last peak for lower frequencies. The prominent peak was defined as the peak with the greatest magnitude. As the frequency increases, the prominent peak shifts towards the first peak. (Figure 4.4).

The phase offset was defined as the percentage of the stroke in which the peak feathering angle occurred. A stroke consists of both an upstroke and a downstroke. A phase

offset of 50% means that the peak feathering angle occurs at mid-stroke, implying that the pitching motion is a half-stroke behind the flapping motion. For a real wing flapping at an average flapping amplitude of  $55^\circ$ , the phase offset of the prominent peak feathering angle reduces as the motion frequency increases, which indicates that the faster the wing flaps the less time it has to passively pitch. Table 4.3 represents the phase offset for each peak for a given input voltage and its corresponding average frequency. It can be seen that the phase offset of the 1<sup>st</sup>, 2<sup>nd</sup>, and 3<sup>rd</sup> peaks increase as the frequency increases.

**Table 4.3: Average phase offset and corresponding average amplitude of each peak for a given input voltage and corresponding average frequency. The \* represents the prominent peak.**

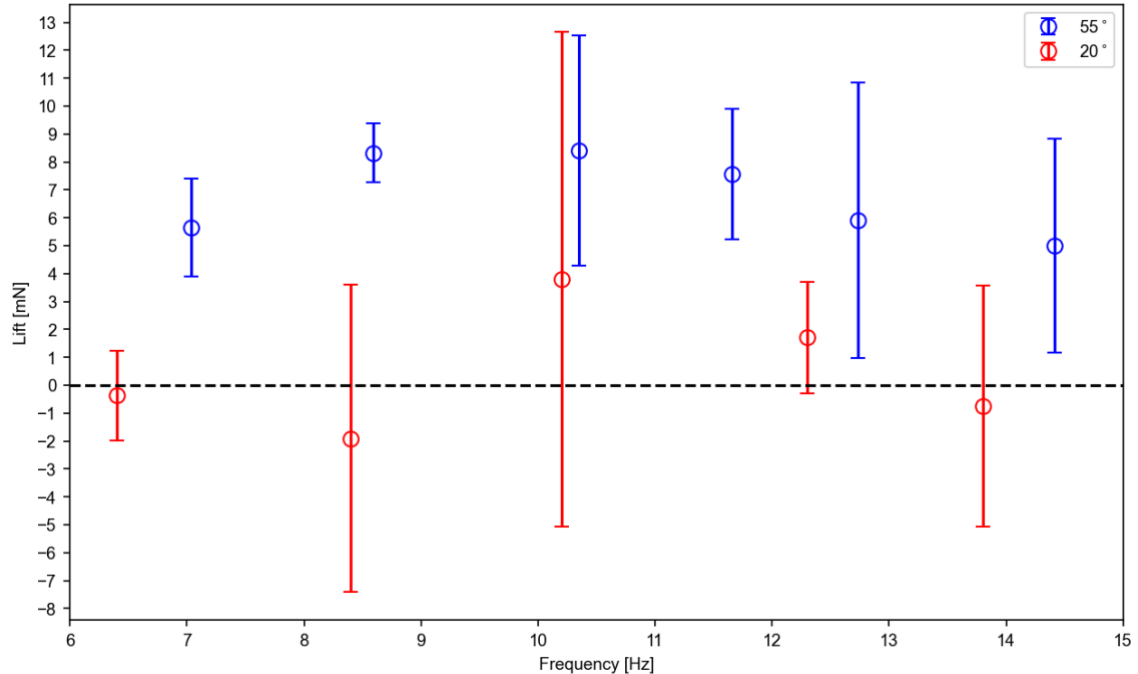
| Volts | Frequency | Average Phase Offset |           |          | Average Amplitude |          |          |
|-------|-----------|----------------------|-----------|----------|-------------------|----------|----------|
|       |           | 1st peak             | 2nd peak  | 3rd peak | 1st peak          | 2nd peak | 3rd peak |
| [V]   | [Hz]      |                      | [%stroke] |          | [deg]             |          |          |
| 0.5   | 7.03      | 28.07                | 41.38*    | 59.05    | 3.51              | 12.16*   | 11.39    |
| 0.6   | 8.59      | 28.62                | 41.38*    | 61.95    | 8.03              | 11.66*   | 8.19     |
| 0.7   | 10.35     | 32.10                | 48.50*    | -        | 9.76              | 13.36*   | -        |
| 0.8   | 11.65     | 32.38                | 57.09*    | -        | 10.18             | 12.93*   | -        |
| 0.9   | 12.73     | 34.67                | 55.30*    | -        | 12.95             | 14.72*   | -        |
| 1     | 14.41     | 32.52*               | -         | -        | 19.39*            | -        | -        |

In Figure 4.3, the data points were generated by taking the average of half the sum of the maximum and minimum feathering angle magnitudes of four trials. The error bars were made to show a 95% confidence interval; however, no outlier analysis was done due to the small sample size. The error for the  $55^\circ$  feathering angle magnitudes was considerably less than error for the  $20^\circ$  feathering angle magnitudes. This is likely due to the data sampling rate for the  $55^\circ$  amplitude cases being significantly greater than those of the  $20^\circ$  cases.

## 4.2 Force Generation by Real Wing

The peak lift generation for the real wing flapping at an average flapping amplitude of  $55^\circ$  occurred at 10.3 Hz (Figure 4.4), which is around the flapping frequency of a monarch in free flight, 10 Hz [54]. The average lift generated at this frequency was 8.4 mN, which is over double the lift generated, 3.8 mN, for a wing flapping at a lower flapping amplitude of  $17.7^\circ$  at a similar frequency of 10.3 Hz [43]. As the total weight of a monarch butterfly is approximately 5 mN [54], the lift generated by just one wing is more than adequate for flight. Furthermore, the lift generated at an average frequency of 7.1 Hz for an average flapping amplitude of  $55^\circ$  is 5.6 mN. This combined with the result of the lift generated by two wings flapping at a much lower amplitude of  $17.7^\circ$  being sufficient to overcome the butterfly's weight [43], suggest that a monarch's flight can have a wide variety of both flapping amplitudes and frequencies that can be used for maneuvering and contribute greatly to the migration of long distances.





**Figure 4.4: Lift forces produced by a monarch wing at 20° and 55° flapping amplitudes for a range of different flapping frequencies. The error bars represent the 95% confidence interval (nred=6, nblue=4).**

In Figure 4.4, the data points were generated by taking the average the maximum recorded lift of four trials at different flapping frequencies. The error bars were made to show a 95% confidence interval; however, no outlier analysis was done due to the small sample size. The error for the lift forces produced at 55° flapping angles was considerably less than error for the 20° flapping angles. This is likely due to the data sampling rate for the 55° cases being significantly greater than those of the 20° cases.

## **Chapter 5. Conclusion**

### **5.1 Conclusion**

The purpose of this study was to determine aeroelastic properties of a monarch butterfly wing near monarch free flight flapping amplitudes. The knowledge gained from these values, feathering angle and phase offset, will allow future butterfly models to be more accurate, furthering future micro-air vehicle development. This study characterized real monarch butterfly wings by measuring the wing angles and force generation. This allowed us to better understand motion of a monarch wing for future fabrication of an artificial wing.

We determined the forces generated by a real monarch wing at 55° flapping amplitudes. The wing produced a peak lift at 10.3 Hz, which corresponds to the flapping frequency of the monarch's standard flight. This correlated well with similar test done at 20° flapping amplitudes. The peak lift measured 8.4 mN, which is over double the peak lift generated at 20° flapping amplitudes. The lift produced, 5.6 mN, at the lowest tested frequency, 7.0 Hz, was more than sufficient to overcome a monarch's average weight, 5 mN. This indicated that a monarch is capable of sustaining flight even outside of its normal flapping frequency of 10 Hz. Furthermore, this lift was produced by one wing, therefore the lift generation of two wing would give the monarch an excess of lift to overcome gust or provide thrust.

## **5.2 Future Work**

Future work on the development of a more realistic bioinspired monarch wing includes the following:

- 1) Repeat the experiments at finer input voltage increments and number of trials for both 20° and 55° cases.
- 2) Measure the wing motion and lift generation of an artificial wing at amplitudes near the free-flight monarch flapping amplitude and compare them to the real wing data.
- 3) Measure lift generation by two real and artificial butterfly wing and compare.
- 4) Measure the wing motion and lift generation on real monarch wings with artificially induced damage or scales removed.
- 5) Investigation of the aerodynamic and viscous damping capabilities of a monarch butterfly wing and their role in wing deformation and force production.
- 6) Measure the aerodynamic characteristics and force generation in a wing-body coupled system.

## **5.3 Acknowledgements**

I would like to thank Madhu Sridhar and Rachel Twigg for all their help during this process. I would like to thank Fredrick Schultz for manufacturing the three-dimensionally printed flapper and mount. And a final thanks to all of the people who provided input and advice during this process.

## References

- [1] Brower, L. P. Monarchs. In *Encyclopedia of Insects*, Elsevier, 2003, pp. 739–743.
- [2] Gibo, D. L. Flight Strategies of Migrating Monarch Butterflies (*Danaus Plexippus* L.) in Southern Ontario. In *Insect Flight*, Springer, Berlin, 1986.
- [3] Shyy, W., Aono, H., Kang, C., and Liu, H. *An Introduction to Flapping Wing Aerodynamics*. Cambridge University Press, New York, 2013.
- [4] Spagnolie, S. E., Moret, L., Shelley, M. J., and Zhang, J. “Surprising Behaviors in Flapping Locomotion with Passive Pitching.” *Physics of Fluids*, Vol. 22, No. 4, 2010, p. 41903.
- [5] Eldredge, J. D., Toomey, J., and Medina, A. “On the Roles of Chord-Wise Flexibility in a Flapping Wing with Hovering Kinematics.” *Journal of Fluid Mechanics*, Vol. 659, 2010, pp. 94–115.
- [6] Wu, P., Stanford, B. K., Sällström, E., Ukeiley, L., and Ifju, P. G. “Structural Dynamics and Aerodynamics Measurements of Biologically Inspired Flexible Flapping Wings.” *Bioinspiration & biomimetics*, Vol. 6, 2011, p. 016009. <https://doi.org/10.1088/1748-3182/6/1/016009>.
- [7] Vargas, A., Mittal, R., and Dong, H. “A Computational Study of the Aerodynamic Performance of a Dragonfly Wing Section in Gliding Flight.” *Bioinspiration & biomimetics*, Vol. 3, No. 2, 2008, p. 26004.
- [8] Dewey, P. A., Boschitsch, B. M., Moored, K. W., Stone, H. A., and Smits, A. J. “Scaling Laws for the Thrust Production of Flexible Pitching Panels.” *Journal of Fluid Mechanics*, Vol. 732, 2013, pp. 29–46.
- [9] Michelin, S., and Llewellyn Smith, S. G. “Resonance and Propulsion Performance

- of a Heaving Flexible Wing.” *Physics of Fluids*, Vol. 21, No. 7, 2009, p. 71902.
- [10] Vanella, M., Fitzgerald, T., Preidikman, S., Balaras, E., and Balachandran, B. “Influence of Flexibility on the Aerodynamic Performance of a Hovering Wing.” *Journal of Experimental Biology*, Vol. 212, No. 1, 2009, pp. 95–105.
- [11] Gordnier, R. E., and Attar, P. J. “Impact of Flexibility on the Aerodynamics of an Aspect Ratio Two Membrane Wing.” *Journal of Fluids and Structures*, Vol. 45, 2014, pp. 138–152.
- [12] Shelley, M. J., and Zhang, J. “Flapping and Bending Bodies Interacting with Fluid Flows.” *Annual Review of Fluid Mechanics*, Vol. 43, 2011, pp. 449–465.
- [13] Alben, S., and Shelley, M. “Coherent Locomotion as an Attracting State for a Free Flapping Body.” *Proceedings of the National Academy of Sciences*, Vol. 102, No. 32, 2005, pp. 11163–11166.
- [14] Quinn, D. B., Lauder, G. V, and Smits, A. J. “Scaling the Propulsive Performance of Heaving Flexible Panels.” *Journal of fluid mechanics*, Vol. 738, 2013, pp. 250–267.
- [15] Masoud, H., and Alexeev, A. “Resonance of Flexible Flapping Wings at Low Reynolds Number.” *Physical Review E*, Vol. 81, No. 5, 2010, p. 56304.
- [16] Shahzad, A., Tian, F.-B., Young, J., and Lai, J. C. S. “Effects of Flexibility on the Hovering Performance of Flapping Wings with Different Shapes and Aspect Ratios.” *Journal of Fluids and Structures*, Vol. 81, 2018, pp. 69–96.
- [17] Kang, C., and Shyy, W. “Scaling Law and Enhancement of Lift Generation of an Insect-Size Hovering Flexible Wing.” *Journal of The Royal Society Interface*, Vol. 10, No. 85, 2013, p. 20130361.

- [18] Yin, B., and Luo, H. “Effect of Wing Inertia on Hovering Performance of Flexible Flapping Wings.” *Physics of Fluids*, Vol. 22, No. 11, 2010, p. 111902.
- [19] Ramanarivo, S., Godoy-Diana, R., and Thiria, B. “Rather than Resonance, Flapping Wing Flyers May Play on Aerodynamics to Improve Performance.” *Proceedings of the National Academy of Sciences*, Vol. 108, No. 15, 2011, pp. 5964–5969.
- [20] Shyy, W., Aono, H., Chimakurthi, S. K., Trizila, P., Kang, C. K., Cesnik, C. E. S., and Liu, H. “Recent Progress in Flapping Wing Aerodynamics and Aeroelasticity.” *Progress in Aerospace Sciences*, Vol. 46, No. 7, 2010, pp. 284–327. <https://doi.org/10.1016/j.paerosci.2010.01.001>.
- [21] Combes, S. A., and Daniel, T. L. “Flexural Stiffness in Insect Wings II. Spatial Distribution and Dynamic Wing Bending.” *Journal of Experimental Biology*, Vol. 206, No. 17, 2003, pp. 2989–2997. <https://doi.org/10.1242/jeb.00524>.
- [22] Combes, S. A., and Daniel, T. L. “Flexural Stiffness in Insect Wings I. Scaling and the Influence of Wing Venation.” *Journal of Experimental Biology*, Vol. 206, No. 17, 2003, pp. 2979–2987. <https://doi.org/10.1242/jeb.00523>.
- [23] Tanaka, H., and Wood, R. J. “Fabrication of Corrugated Artificial Insect Wings Using Laser Micromachined Molds.” *Journal of Micromechanics and Microengineering*, Vol. 20, No. 7, 2010, p. 75008.
- [24] Stepan, S. J. “Flexural Stiffness Patterns of Butterfly Wings (Papilionoidea).” *Journal of Research on the Lepidoptera*, Vol. 35, 1996, pp. 61–77.
- [25] Donoughe, S., Crall, J. D., Merz, R. A., and Combes, S. A. “Resilin in Dragonfly and Damselfly Wings and Its Implications for Wing Flexibility.” *Journal of*

- Morphology*, Vol. 272, 2011, pp. 1409–1421. <https://doi.org/10.1002/jmor.10992>.
- [26] Brower, L. P. “Monarch Butterfly Orientation: Missing Pieces of a Magnificent Puzzle.” *The Journal of experimental biology*, Vol. 199, No. Pt 1, 1996, pp. 93–103.
- [27] Brower, L. P., Fink, L. S., and Walford, P. “Fueling the Fall Migration of the Monarch Butterfly.” *Integrative and Comparative Biology*, Vol. 46, No. 6, 2006, pp. 1123–1142. <https://doi.org/10.1093/icb/icl029>.
- [28] Froy, O., Gotter, A. L., Casselman, A. L., and Reppert, S. M. “Illuminating the Circadian Clock in Monarch Butterfly Migration.” *Science*, Vol. 300, 2003, pp. 1303–1306.
- [29] Merlin, C., Gegear, R. J., and Reppert, S. M. “Sun Compass Orientation in Migratory.” *Cycle*, Vol. 325, No. 6, 2009, pp. 1700–1705.
- [30] Wassenaar, L. I., and Hobson, K. A. “Natal Origins of Migratory Monarch Butterflies at Wintering Colonies in Mexico : New Isotopic Evidence.” *Proceedings of the National Academy of Sciences*, Vol. 95, No. December, 1998, pp. 15436–15439.
- [31] Urquhart, F. A., and Urquhart, N. R. “The Overwintering Site of the Eastern Population of the Monarch Butterfly (*Danaus p. Plexippus*; *Danaidae*) in Southern Mexico.” *Journal of the Lepidopterists’ Society*, Vol. 30, No. 3, 1976, pp. 153–158.
- [32] Reppert, S. M., and Roode, J. C. De. “Demystifying Monarch Butterfly Migration.” *Current Biology*, Vol. 28, 2018, pp. R1009–R1022. <https://doi.org/10.1016/j.cub.2018.02.067>.
- [33] Slayback, D. A., Brower, L. P., Ramírez, M. I., and Fink, L. S. “Establishing the Presence and Absence of Overwintering Colonies of the Monarch Butterfly in

- Mexico by the Use of Small Aircraft.” *American Entomologist*, Vol. 53, No. 1, 2007, pp. 28–40.
- [34] Masters, A. R., Malcolm, S. B., and Brower, L. P. “Monarch Butterfly (*Danaus Plexippus*) Thermoregulatory Behavior and Adaptations for Overwintering in Mexico.” *Ecology*, Vol. 69, No. 2, 1988, pp. 458–467.
- [35] Nakata, T., Liu, H., Tanaka, Y., Nishihashi, N., Wang, X., and Sato, A. “Aerodynamics of a Bio-Inspired Flexible Flapping-Wing Micro Air Vehicle.” *Bioinspiration & biomimetics*, Vol. 6, No. 4, 2011, p. 45002.
- [36] Wootton, R. J. “Support and Deformability in Insect Wings.” *Journal of Zoology, London*, Vol. 193, 1981, pp. 447–468.
- [37] Sridhar, M., Kang, C.-K., and Landrum, D. B. Beneficial Effect of the Coupled Wing-Body Dynamics on Power Consumption in Butterflies. 2019.
- [38] Song, F., Lee, K. L., Soh, A. K., Zhu, F., and Bai, Y. L. “Experimental Studies of the Material Properties of the Forewing of Cicada (Homóptera, Cicàdidae).” *Journal of Experimental Biology*, Vol. 207, 2004, pp. 3035–3042. <https://doi.org/10.1242/jeb.01122>.
- [39] Wainwright, S. A., Biggs, W. D., Gosline, J. M., and Currey, J. D. *Mechanical Design in Organisms*. Princeton University Press, 1976.
- [40] Jensen, M., and Weis-Fogh, T. “Biology and Physics of Locust Flight. V. Strength and Elasticity of Locust Cuticle.” *Philosophical Transactions of the Royal Society B: Biological Sciences*, Vol. 245, No. 721, 1962, pp. 137–169.
- [41] Lietz, C., Schaber, C. F., Gorb, S. N., and Rajabi, H. “The Damping and Structural Properties of Dragonfly and Damselfly Wings during Dynamic Movement.”

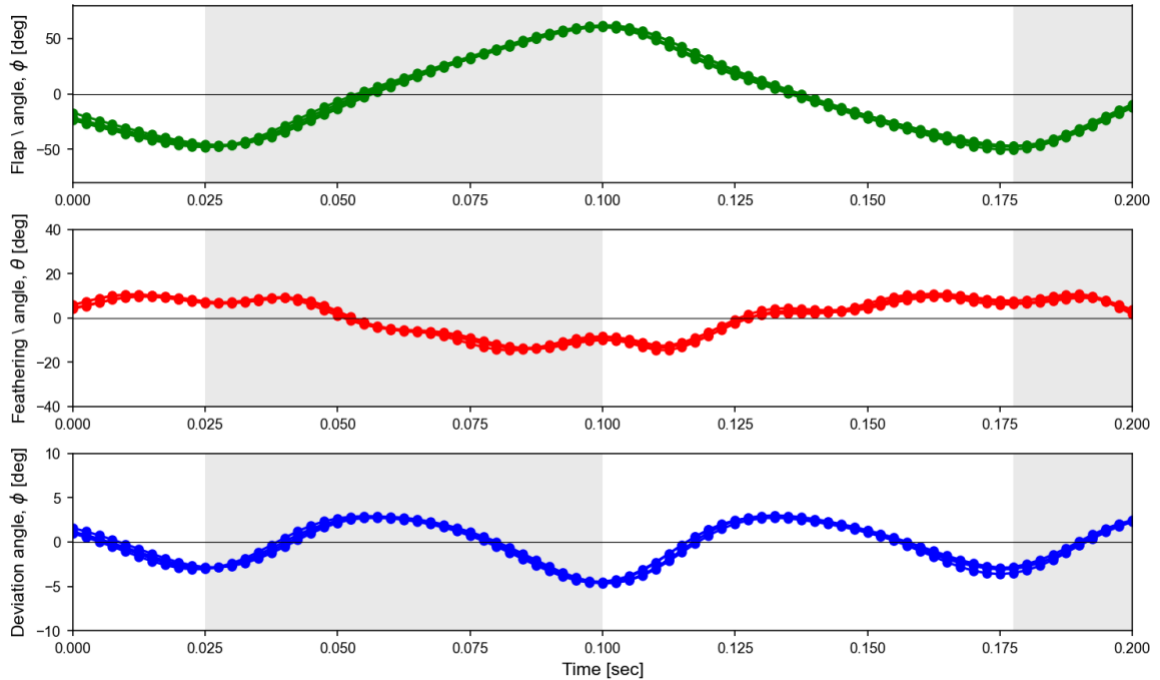


- Communications Biology*, Vol. 4, No. 1, 2021. <https://doi.org/10.1038/s42003-021-02263-2>.
- [42] Cheng, B., and Deng, X. “Translational and Rotational Damping of Flapping Flight and Its Dynamics and Stability at Hovering.” *IEEE Transactions on Robotics*, Vol. 27, No. 5, 2011, pp. 849–864. <https://doi.org/10.1109/TRO.2011.2156170>.
- [43] Twigg, R., Sridhar, M. K., Pohly, J., Hildebrant, N., Kang, C. K., Landrum, D. B., Roh, K. H., and Salzwedel, S. “Aeroelastic Characterization of Real and Artificial Monarch Butterfly Wings.” *AIAA Scitech 2020 Forum*, Vol. 1 PartF, 2020. <https://doi.org/10.2514/6.2020-2002>.
- [44] Davis, A. K., Farrey, B. D., and Altizer, S. “Variation in Thermally Induced Melanism in Monarch Butterflies (Lepidoptera: Nymphalidae) from Three North American Populations.” *Journal of Thermal Biology*, Vol. 30, 2005, pp. 410–421. <https://doi.org/10.1016/j.jtherbio.2005.04.003>.
- [45] Mccord, J. W., and Davis, A. K. “Biological Observations of Monarch Butterfly Behavior at a Migratory Stopover Site : Results from a Long-Term Tagging Study in Coastal South Carolina.” 2010, pp. 405–418. <https://doi.org/10.1007/s10905-010-9224-x>.
- [46] James, D. Thermoregulation in *Danaus Plexippus* (L.) (Lepidoptera: Nymphalidae): Two Cool Climate Adaptations. 43–47.
- [47] Ffrench-Constant, R. H. “Of Monarchs and Migration.” *Nature*, Vol. 514, No. 7522, 2014, pp. 314–315. <https://doi.org/10.1038/514283a>.
- [48] Gibo, D. L. “Altitudes Attained By Migrating Monarch Butterflies, *Danaus P. Plexippus* (Lepidoptera: Danainae), as Reported By Glider Pilots.” *Canadian*

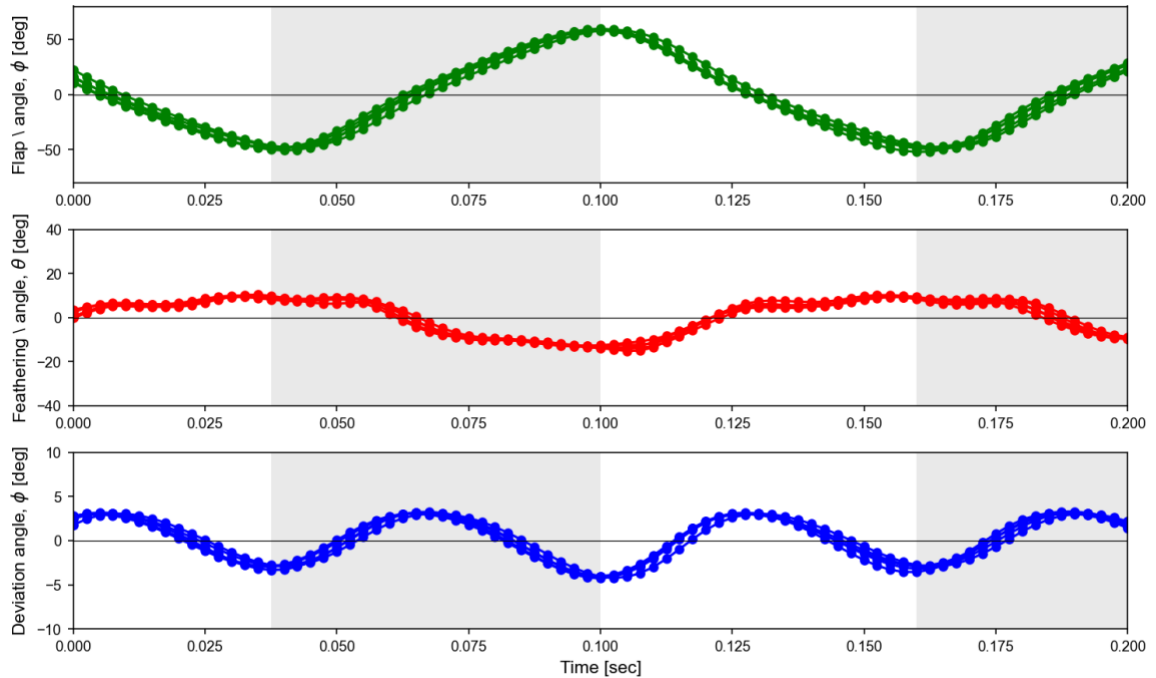
- Journal of Zoology*, Vol. 59, No. 3, 1981, pp. 571–572. <https://doi.org/10.1139/z81-084>.
- [49] Gibo, D. L., and Pallett, M. J. “Soaring Flight of Monarch Butterflies, *Danaus Plexippus* (Lepidoptera: Danaidae), during the Late Summer Migration in Southern Ontario.” *Canadian Journal of Zoology*, Vol. 57, 1979, pp. 1393–1401. <https://doi.org/10.1139/z79-180>.
- [50] Paoletti, P., and Mahadevan, L. “Intermittent Locomotion as an Optimal Control Strategy.” *Proceedings of the Royal Society A*, Vol. 470, No. January, 2014, p. 20130535.
- [51] Song, F., Xiao, K. W., Bai, K., and Bai, Y. L. “Microstructure and Nanomechanical Properties of the Wing Membrane of Dragonfly.” *Materials Science & Engineering A*, Vol. 457, 2007, pp. 254–260. <https://doi.org/10.1016/j.msea.2007.01.136>.
- [52] Klocke, D., and Schmitz, H. “Water as a Major Modulator of the Mechanical Properties of Insect Cuticle.” *Acta Biomaterialia*, Vol. 7, 2011, pp. 2935–2942. <https://doi.org/10.1016/j.actbio.2011.04.004>.
- [53] Micron Wings.
- [54] Kang, C. K., Cranford, J., Sridhar, M. K., Kodali, D., Landrum, D. B., and Slegers, N. “Experimental Characterization of a Butterfly in Climbing Flight.” *AIAA Journal*, Vol. 56, No. 1, 2018, pp. 15–24. <https://doi.org/10.2514/1.J055360>.
- [55] Sridhar, M. K., Kang, C. K., and Lee, T. “Geometric Formulation for the Dynamics of Monarch Butterfly with the Effects of Abdomen Undulation.” *AIAA Scitech 2020 Forum*, Vol. 1 PartF, No. January, 2020, pp. 1–24. <https://doi.org/10.2514/6.2020-1962>.

## Appendix A

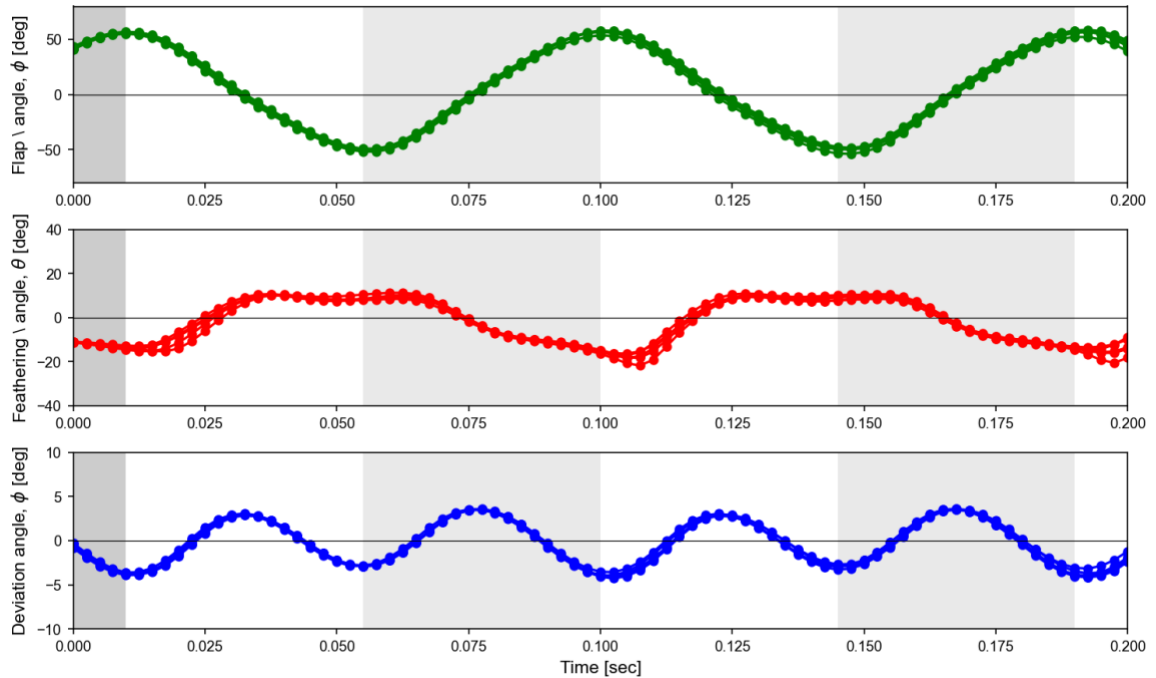
### Additional Wing Angle Figures



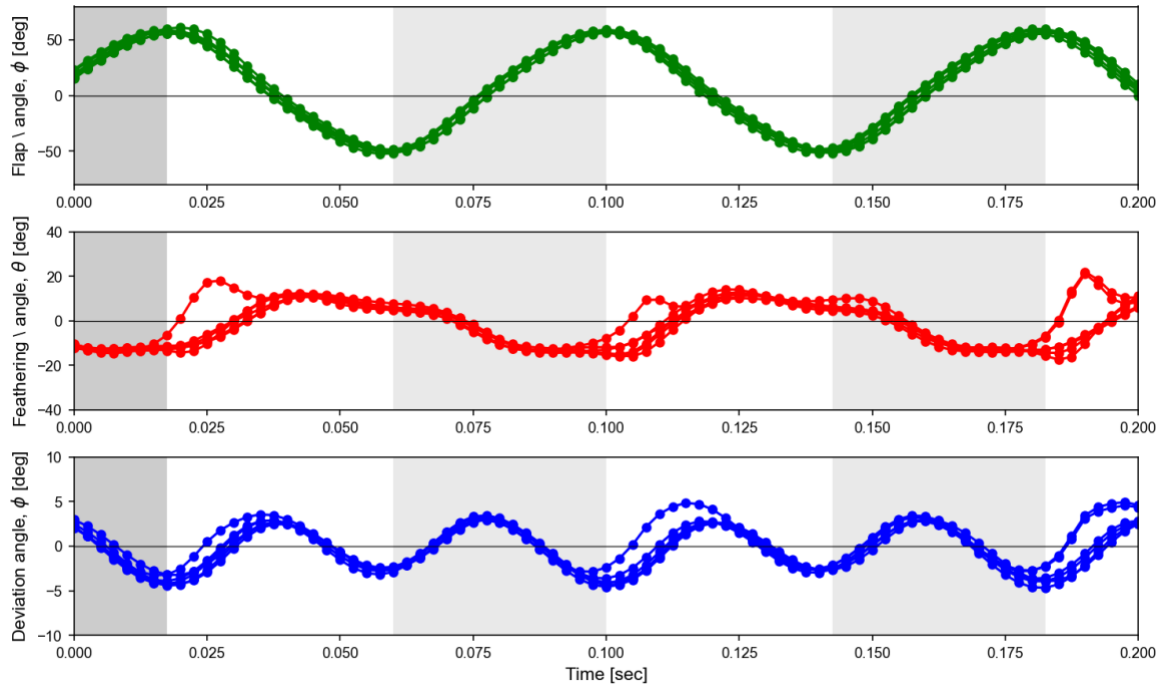
**Figure A.1: Representative time histories of the flapping angle, feathering angle, and deviation angle of a real monarch butterfly wing mounted on the gearbox and operated at an input voltage of 0.5 V. The FFT analysis of the flapping motion indicates that the flapping frequency was 7 Hz. The grey bars indicate the downstroke, and the white bars indicate the upstroke. \*The original data was shifted to be symmetric about the x-axis.**



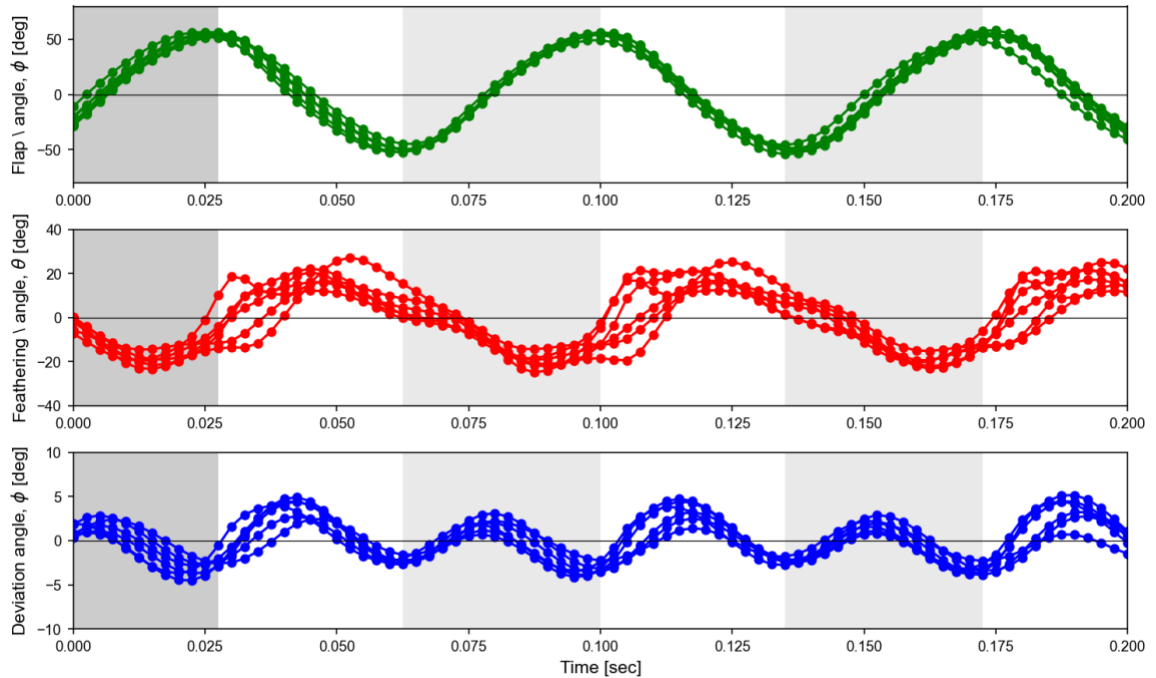
**Figure A.2: Representative time histories of the flapping angle, feathering angle, and deviation angle of a real monarch butterfly wing mounted on the gearbox and operated at an input voltage of 0.6 V. The FFT analysis of the flapping motion indicates that the flapping frequency was 8.6 Hz. The grey bars indicate the downstroke, and the white bars indicate the upstroke. \*The original data was shifted to be symmetric about the x-axis.**



**Figure A.3: Representative time histories of the flapping angle, feathering angle, and deviation angle of a real monarch butterfly wing mounted on the gearbox and operated at an input voltage of 0.8 V. The FFT analysis of the flapping motion indicates that the flapping frequency was 11.7 Hz. The grey bars indicate the downstroke, and the white bars indicate the upstroke. \*The original data was shifted to be symmetric about the x-axis.**



**Figure A.4: Representative time histories of the flapping angle, feathering angle, and deviation angle of a real monarch butterfly wing mounted on the gearbox and operated at an input voltage of 0.9 V. The FFT analysis of the flapping motion indicates that the flapping frequency was 12.7 Hz. The grey bars indicate the downstroke, and the white bars indicate the upstroke. \*The original data was shifted to be symmetric about the x-axis.**



**Figure A.5: Representative time histories of the flapping angle, feathering angle, and deviation angle of a real monarch butterfly wing mounted on the gearbox and operated at an input voltage of 1.0 V. The FFT analysis of the flapping motion indicates that the flapping frequency was 14.4 Hz. The grey bars indicate the downstroke, and the white bars indicate the upstroke. \*The original data was shifted to be symmetric about the x-axis.**